



# Rapid In-Situ Stress Measurement in Vertical Borehole Based on Borehole Diametrical Deformation Analysis

Chao Wang<sup>1,2</sup> · Zengqiang Han<sup>1,2</sup> · Yiteng Wang<sup>1</sup> · Chuanying Wang<sup>1</sup> · Jinchao Wang<sup>1</sup> · Sheng Hu<sup>1</sup>

Received: 19 December 2022 / Accepted: 17 July 2023 / Published online: 16 August 2023  
© The Author(s), under exclusive licence to Springer-Verlag GmbH Austria, part of Springer Nature 2023

## Abstract

In-situ stress measurement is an important prerequisite for underground engineering excavation design and surrounding rock stability analysis. However, it is still a difficult problem to complete in-situ stress measurement quickly and accurately, especially in deep vertical borehole with more complex environment. Aiming at the existing problems, a new in-situ stress measurement method is proposed in this study. The principle of in-situ stress calculation based on the borehole diametrical deformation analysis is established, and a borehole diametrical deformation measurement equipment which can realize the directional measurement of multi-directional borehole wall displacement is developed according to this principle. The traditional single action double-tube drilling tool is optimized, and the corresponding in-situ stress measurement process is formulated, forming a rapid in-situ stress measurement method with the cooperation of drilling tools. The measurement method has been applied to the in-situ stress measurement at – 410 m and – 500 m levels in Zhangfushan deposit of Jinshandian Iron Mine, and effective diametrical deformation data of 6 measuring points were obtained. The measurement results show that the optimized single action double-tube drilling tool has the ability of accurate drilling and complete coring, and can assist in the rapid measurement of in-situ stress. The principal stress at the 6 measuring points basically increases with the increase of depth, and the direction of the maximum horizontal principal stress is about SN, which is basically consistent with the existing in-situ stress data. The results show that the method proposed in this paper can realize the rapid and accurate measurement of in-situ stress in vertical borehole.

## Highlights

- A principle for calculating in-situ stress based on the analysis of diametrical deformation characteristics of boreholes has been established.
- A device has been developed that can measure diametrical displacement of borehole in multiple directions.
- The method was used for in-situ measurement and the accuracy of the measurement results was verified through historical data.

**Keywords** In-situ stress measurement · Borehole diametrical deformation · Borehole cross-sectional shape · Diametrical deformation measurement equipment · Double-tube drilling tool

## 1 Introduction

In-situ stress is the natural stress existing in the stratum without engineering disturbance, and it is one of the most important parameters in rock mass engineering (Vazaios et al. 2019; Li 2021; Layer 1997). With the economic development and the increasing demand for resource exploitation, underground engineering has gradually moved towards the deep, and the operation depth in the fields of hydro-power, geothermal, mineral, oil and gas has reached several

✉ Zengqiang Han  
zqhan@whrsm.ac.cn

<sup>1</sup> State Key Laboratory of Geomechanics and Geotechnical Engineering, Institute of Rock and Soil Mechanics, Chinese Academy of Sciences, Wuhan 430071, Hubei, China

<sup>2</sup> University of Chinese Academy of Sciences, Beijing 100049, China

kilometers (Pang et al. 2015; Zhang et al. 2016; Xie et al. 2019). In deep engineering, high in-situ stress exists widely, which seriously threatens the safety of engineering construction projects (Oreste 2005; Li et al. 2014; Ptacek et al. 2015; Feng et al. 2019). Therefore, accurate in-situ stress measurement is a prerequisite for underground engineering construction.

The in-situ stress measurement methods mainly include stress relief method (Sjöberg et al. 2003; Mukai et al. 2007), hydraulic fracturing method (Haimson and Cornet 2003; Liu et al. 2014; Xu et al. 2016), borehole breakout method (Zhang et al. 2018; Han et al. 2020a), flat jack method (He and Hatzor 2015; Mckenney and Corkum 2020), strain recovery method (Byrne et al. 2009; Sun et al. 2014; Nagano et al. 2015), and acoustic emission method (Lehtonen et al. 2012; Bai et al. 2018). Among them, the stress relief method is widely recognized, and is also one of the in-situ stress measurement methods suggested by ISRM (Sjöberg et al. 2003). The typical measurement techniques include USBM diametrical deformation gauge developed by the U.S. Bureau of mines (Merrill 1967), CSIR triaxial strain gauge developed by the scientific and Industrial Research Commission of South Africa (Leeman 1971), CSIRO hollow inclusion triaxial strain gauge made by the federal scientific and industrial research organization of Australia (Sjöberg and Klasson 2003). However, the traditional stress relief measurement technology is mainly used in shallow boreholes, but there are many limitations in the application of deep vertical boreholes. The main reasons are: (1) the possible high temperature and high water pressure environment seriously affects the reliability of electronic strain gauges (Cai et al. 1995, 2000); (2) the strain gauge data are usually transmitted to the ground through the wire, and the wire layout in the deep borehole is more difficult and unreliable; (3) the hardening of epoxy resin takes a long time (Sjöberg and Klasson 2003; Lahaie et al. 2010; Li et al. 2019). In order to meet the needs of deep borehole measurement, many scholars have carried out fruitful research. Ge and Hou (2012) proposed the three-dimensional in-situ stress measurement method of borehole wall stress relief method (BWSRM) and applied it to the in-situ stress measurement at the buried depth of 2430 m of Jinping II hydropower station. Bai et al. (2013) developed a deep hole hollow inclusion in-situ stress measuring instrument, which integrates strain gauge, stress gauge, electronic compass, pressure sensor and thermometer, and overcomes the difficulties caused by wires in deep boreholes. Li et al. (2019) developed CSIRO cell with the compromised application of instantaneous data-logging, no-power data-connection and twin temperature compensation techniques, it has good test accuracy and acquisition system stability. However, these studies do not completely solve the problem of rapid and accurate

measurement of in-situ stress in complex deep borehole environment.

Aiming at the existing problems, a rapid in-situ stress measurement method suitable for vertical deep borehole is developed in this paper. The relationship between borehole diametrical deformation analysis and in-situ stress calculation is established, and the borehole diametrical deformation measurement equipment is developed. The equipment solves the problems of deep vertical hole measurement such as great influence of high temperature and high pressure, difficult data transmission and inconvenient equipment installation, and realizes multi-directional diametrical deformation measurement. In addition, the single acting double-tube drilling tool is optimized to complete the downhole tasks of accurate borehole forming and complete coring, and assist in the rapid measurement of in-situ stress; The measurement method has been applied to the in-situ stress measurement at  $-410$  m and  $-500$  m levels in Jinshandian Iron Mine, and reliable in-situ stress measurement data have been obtained.

## 2 Concept and Theory

### 2.1 Borehole Diametrical Deformation Under In-Situ Stress

The analysis of borehole diametrical deformation is based on the theory of elasticity, assuming that the rock mass is an infinite elastic body, and the borehole is elastically deformed under the action of far-field stress. Taking the center of the borehole as the origin of the coordinate and the direction of the far-field principal stress as  $x$ -axis and  $y$ -axis, the  $xoy$  coordinate system was established. The stress state of borehole is shown in Fig. 1,  $\sigma_1$  and  $\sigma_2$  are the maximum and minimum principal stresses in the plane, respectively. A, B and C are

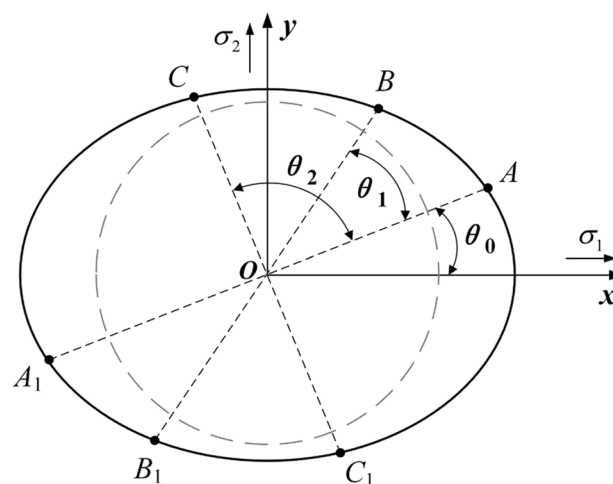


Fig. 1 Schematic diagram of diametrical deformation and stress state

the three points on the borehole wall, while  $A_1$ ,  $B_1$ , and  $C_1$  are the symmetrical points of A, B and C about the center of the borehole.  $\theta_0$  is the angle between  $AA_1$  and the  $x$ -axis,  $\theta_1$  is the angle between  $BB_1$  and  $AA_1$ , and  $\theta_2$  is the angle between  $CC_1$  and  $AA_1$ .

According to the theory of elasticity, the relationship between diametrical displacement and stress of any point A on the hole wall can be expressed as Eq. (1), and the relationship between tangential displacement and stress can be expressed as Eq. (2) (Han et al. 2020b):

$$\begin{cases} u_1 = \frac{\sigma_1 d(1-\mu^2)}{2E} (1 + 2\cos 2\theta_0) \\ u_2 = \frac{\sigma_2 d(1-\mu^2)}{2E} (1 - 2\cos 2\theta_0) \end{cases} \quad (1)$$

$$\begin{cases} v_1 = -\frac{\sigma_1 d(1-\mu^2)}{2E} \sin 2\theta_0 \\ v_2 = \frac{\sigma_2 d(1-\mu^2)}{2E} \sin 2\theta_0 \end{cases} \quad (2)$$

where  $u_1$  and  $u_2$  are the diametrical displacement of point A on hole wall under the action of  $\sigma_1$  and  $\sigma_2$ , respectively.  $v_1$  and  $v_2$  are the tangential displacement of point A, respectively.  $d$  is the diameter of hole.  $\mu$  is Poisson's ratio.  $E$  is the elastic modulus.

According to the superposition principle, the diametrical displacement  $u$  and tangential displacement  $v$  of point A under the combined action of  $\sigma_1$  and  $\sigma_2$  can be expressed as Eqs. (3) and (4):

$$u = u_1 + u_2 = \frac{d(1-\mu^2)}{2E} [\sigma_1 + \sigma_2 + 2(\sigma_1 - \sigma_2)\cos 2\theta_0] \quad (3)$$

$$v = v_1 + v_2 = -\frac{d(1-\mu^2)}{2E} [2(\sigma_1 - \sigma_2)\sin 2\theta_0] \quad (4)$$

The displacement of points on the wall of a circular hole is symmetric, so the diametrical deformation  $U$  of the circular hole under the combined action of  $\sigma_1$  and  $\sigma_2$  can be expressed as Eq. (5):

$$U = 2u = \frac{d(1-\mu^2)}{E} [\sigma_1 + \sigma_2 + 2(\sigma_1 - \sigma_2)\cos 2\theta_0] \quad (5)$$

Assuming that  $AA_1$ ,  $BB_1$  and  $CC_1$  are any three aperture directions,  $U_1$ ,  $U_2$  and  $U_3$  are the diametrical deformation in these three directions, respectively. The relationship between the amount of diametrical deformation in any three directions and the in-situ stress is established, which can be expressed as Eq. (6):

$$\begin{cases} U_1 = \frac{d(1-\mu^2)}{E} [(\sigma_1 + \sigma_2) + 2(\sigma_1 - \sigma_2)\cos 2\theta_0] \\ U_2 = \frac{d(1-\mu^2)}{E} [(\sigma_1 + \sigma_2) + 2(\sigma_1 - \sigma_2)\cos(2\theta_0 + 2\theta_1)] \\ U_3 = \frac{d(1-\mu^2)}{E} [(\sigma_1 + \sigma_2) + 2(\sigma_1 - \sigma_2)\cos(2\theta_0 + 2\theta_2)] \end{cases} \quad (6)$$

According to Eq. (5), a group of maximum principal stress value, minimum principal stress value and principal stress direction can be calculated by the combination of diametrical deformation in any three directions and angle relation.

### 2.2 Cross-sectional Shape After Borehole Deformed

According to the analysis of the cross-sectional shape after borehole deformation in Fig. 1, under the  $xoy$  coordinate system, the coordinates of any point A(x,y) on the borehole wall can be expressed as Eq. (7):

$$\begin{cases} x = \frac{d}{2}\cos\theta + u\cos\theta - v\sin\theta \\ y = \frac{d}{2}\sin\theta + u\sin\theta + v\cos\theta \end{cases} \quad (7)$$

Substituting Eqs. (3) and (4) into Eq. (7), the following can be obtained:

$$\begin{cases} x = \frac{d}{2} \left[ 1 + \frac{(1-\mu^2)}{E} \cdot (3\sigma_1 - \sigma_2) \right] \cos\theta \\ y = \frac{d}{2} \left[ 1 + \frac{(1-\mu^2)}{E} \cdot (3\sigma_2 - \sigma_1) \right] \sin\theta \end{cases} \quad (8)$$

Let:

$$\begin{cases} A_0 = \frac{d}{2} \left[ 1 + \frac{(1-\mu^2)}{E} \cdot (3\sigma_1 - \sigma_2) \right] \\ B_0 = \frac{d}{2} \left[ 1 + \frac{(1-\mu^2)}{E} \cdot (3\sigma_2 - \sigma_1) \right] \end{cases} \quad (9)$$

Then, Eq. (8) can be expressed as

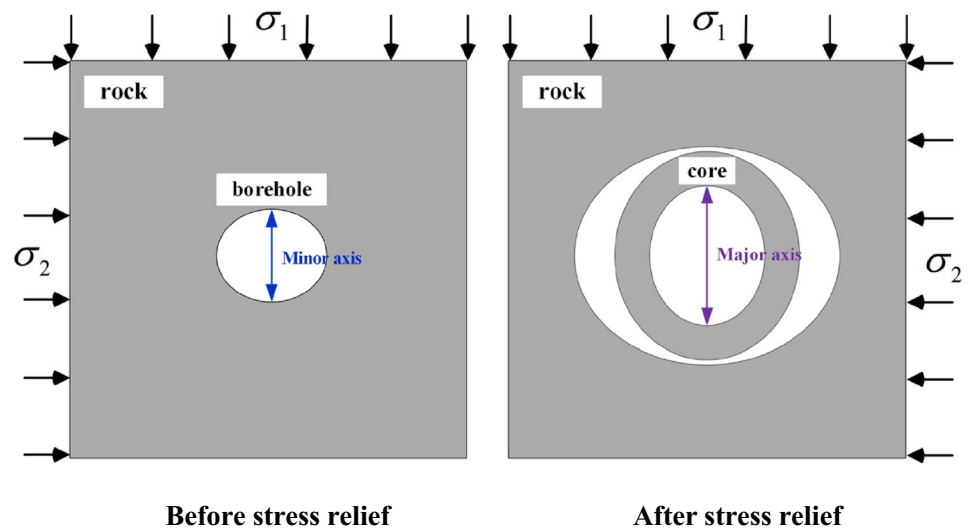
$$\begin{cases} x = A_0\cos\theta \\ y = B_0\sin\theta \end{cases} \quad (10)$$

Satisfy the standard ellipse equation:

$$\frac{x^2}{A_0^2} + \frac{y^2}{B_0^2} = \cos^2\theta + \sin^2\theta = 1 \quad (11)$$

where  $A_0$  and  $B_0$  are the semimajor and semiminor axis of the ellipse, respectively. It is proved that under the plane stress state, the borehole deforms from circle to ellipse, and the direction of ellipse axis coincides with the direction of far-field principal stress. Therefore,  $\sigma_1$  and  $\sigma_2$  can be expressed as

**Fig. 2** Relationship between cross-section shape and principal stress of borehole and core before and after stress relief



$$\begin{cases} \sigma_1 = \frac{3A_0 + B_0 - 2d}{4d} \cdot \frac{E}{(1 - \mu^2)} \\ \sigma_2 = \frac{A_0 + 3B_0 - 2d}{4d} \cdot \frac{E}{(1 - \mu^2)} \end{cases} \quad (12)$$

In addition, the differential stress  $S$  can be expressed as

$$S = \sigma_1 - \sigma_2 = \frac{A_0 - B_0}{2d} \cdot \frac{E}{(1 - \mu^2)} \quad (13)$$

According to Eqs. (12) and (13), the maximum principal stress, minimum principal stress and differential stress in the plane can be calculated by obtaining the ellipse shape parameters (including semimajor axis, semiminor axis and axis direction) after borehole deformation, and the ellipse axis direction is the principal stress direction.

In plane strain state, the geometry of borehole section and core section will change from circle to ellipse after stress relief, and the morphological characteristics of ellipse are related to the direction of principal stress (Han et al. 2020b). The minor axis of borehole section ellipse before stress relief and the major axis of core section ellipse after stress relief represent the direction of maximum principal stress, as shown in Fig. 2. Therefore, the direction of the principal stress can be quickly determined by measuring the elliptical axis direction of the borehole or core section after stress relief, and the physical parameters of the rock are not used in this process. However, if it is necessary to determine the magnitude of the principal stress, the physical parameters of the rock are still required.

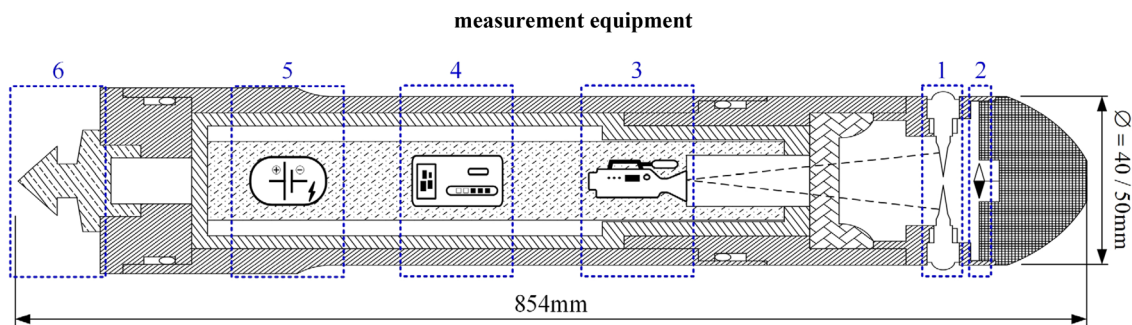


**Fig. 3** Structural diagram of contact type micro-optical borehole diametrical deformation measurement equipment. **1** Diametrical deformation sensing part for transmitting diametrical deformation of hole walls. **2** Azimuth measurement part for measuring the azimuth of rigid contact pins. **3** Optical microscopic imaging part for capturing rigid contact pins displacement. **4** Data processing module for over-

laying and storing video and azimuth data. **5** Power supply for providing energy to internal electronic components. **6** Spear for installing measurement equipment in the hole. The measurement equipment is 854 mm long and has two diameters of 40 mm and 50 mm to meet different measurement requirements

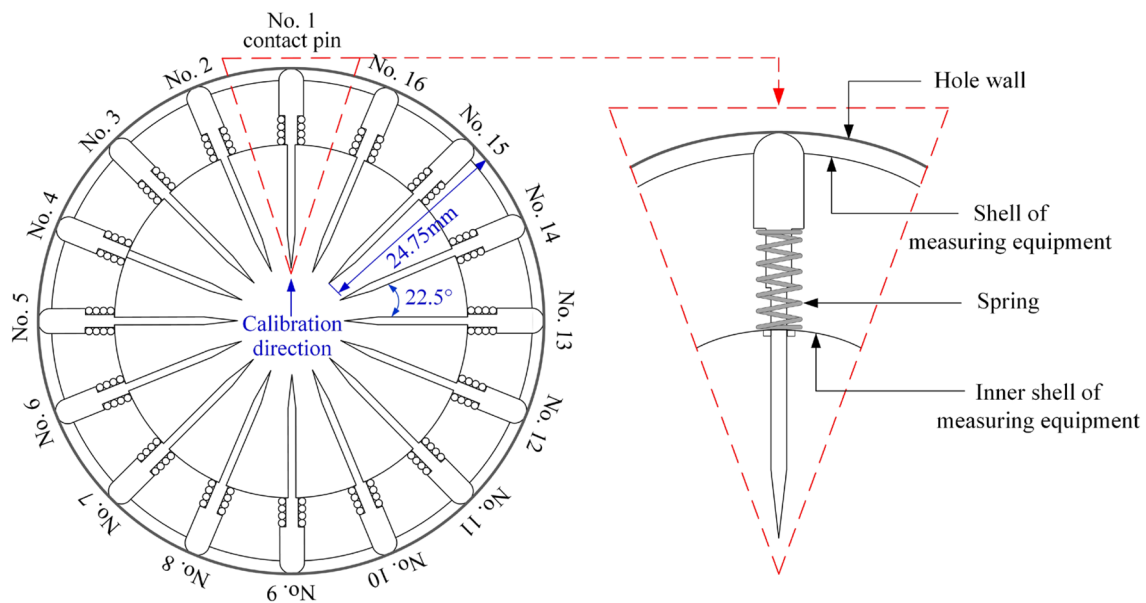


**Fig. 4** Schematic diagram of diametrical deformation sensing part. This part mainly consists of 16 rigid contact pins arranged evenly in the same plane. Under the action of the spring, the pins adheres tightly to the hole wall and moves synchronously

### 3 Development of Measurement Equipment

#### 3.1 Borehole Diametrical Deformation Measurement Equipment

Based on diametrical deformation sensing, micro-optical imaging and azimuth measurement technology, a contact micro-optical borehole diametrical deformation measurement equipment is developed (Wang et al. 2018). This equipment can continuously obtain and visualize the borehole diameter change during stress relief process, and the main parts of the equipment include diametrical deformation sensing, azimuth measurement, optical microscopic imaging, data processing module, power supply and spear. The equipment structure is shown in Fig. 3.

- (1) The diametrical deformation sensing part adopts multiple groups of rigid contact pins symmetrically arranged to reflect the change of diameter. The length of each rigid contact pins is 24.75 mm, and the angle between adjacent pins is  $22.5^\circ$ , as shown in Fig. 4. The rigid contact pins are installed between the outer shell and inner shell of the measurement equipment. When the spring is in its natural state, the contact end protrudes 1.25 mm from the outer shell, which means the diametrical deformation measurement range is 2.5 mm. Assuming the diameter of the measurement equipment is 40 mm, the suitable measuring hole diameter range is 40–42.5 mm. After the measurement equipment is installed in the measuring hole, the spring is in a compressed state. Under the action of the spring, the contact end is tightly attached to the hole wall and moves synchronously with the hole wall. There is no need to inject glue between the contact end and the hole wall, greatly reducing the measurement time of in-situ stress. The design of multiple sets of contact pins enables the equipment to obtain rich data of hole diametrical deformation, which guarantees the screening and optimization of in-situ stress calculation results. Similar to other stress relief equipment, this measurement equipment can only be applied in intact rocks. In addition, it is best to ensure that the hole wall is smooth and complete, but when the small defects on the hole wall are still within the measurement range of the contact pins, the measurement data are also reliable. This may affect the fitting accuracy of the cross-sectional shape of the measuring hole, but the stress state can still be calculated through the diametrical deformation and angle relationship of the hole in any three directions.
- (2) The azimuth measurement part adopts an electronic compass with an accuracy of  $0.1^\circ$ . In addition, adjust the electronic compass  $0^\circ$  and No. 1 contact pin to the true north direction, that is, the reading of the electronic compass indicates the clockwise rotation angle of No. 1 contact pin from the north. The azimuth of other pins can be calculated based on the angle relationship.
- (3) The optical micro-imaging part adopts Charge Coupled Device (CCD) camera. CCD is a semiconductor chip that can convert optical images into digital signals. The



cameras made with CCD chips have the characteristics of small size and light weight (Segawa et al. 1995). During the stress relief process, the CCD camera captures the rigid needle tip and forms a video file, which records the displacement information of the hole wall transmitted by the needle tip. The physical resolution of the collected image can reach 0.003 mm, which greatly ensures the accuracy of in-situ stress measurement results.

- (4) The data processing module is responsible for in-situ processing and storing video images and azimuth data. To ensure the time synchronization between azimuth data and video data, azimuth data are superimposed onto the video image. Each frame of the superimposed image contains the displacement and azimuth information of the hole wall at that time. The measurement data are processed and stored inside the equipment, avoiding the trouble caused by long-distance transmission cables.
- (5) The power supply is built into the measurement equipment and can be cycled for charging. The fully charged state ensures that the measurement equipment can work continuously for at least 6 h.
- (6) The spear can be connected with the conventional fishing tools in the geological drilling industry, and the measurement equipment can be installed into the crustal stress measuring hole through the fishing tools.

All parts of the equipment are made of non-magnetic materials. The equipment shell is made of stainless steel with a wall thickness of 4 mm, which can withstand 15 MPa water pressure without structural damage. The maximum heat-resistant temperature of internal electronic components can reach 100 °C, and thermal insulation tiles are also equipped to further ensure the normal operation of internal components in high-temperature environment.

### 3.2 Auxiliary Equipment for In-Situ Stress Measurement

In-situ stress measurement by stress relief method must be carried out in intact rock, so the core should not be damaged by external forces during coring. In addition, the measuring range of the contact type micro-optical diametrical deformation measurement equipment is 2.5 mm. If the diameter error of the measuring hole is too large, the measurement equipment cannot be successfully installed. Therefore, complete rock cores and high-quality measurement holes are crucial. Double-tube drilling tools (Tang et al. 2009; Talalay 2014) are commonly used in the geological drilling industry to improve the coring rate, especially single acting double-tube drilling tools that do not

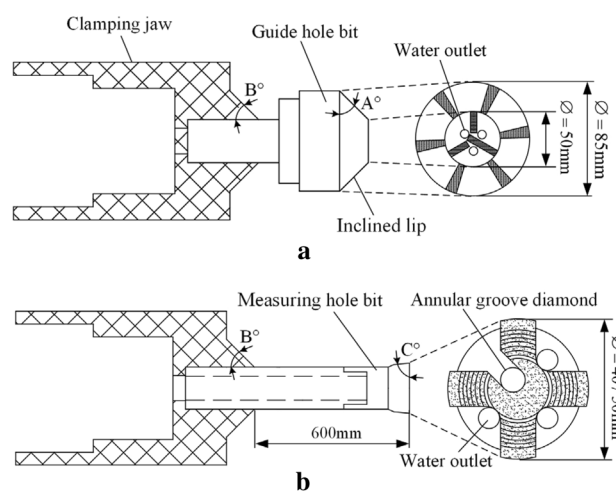


**Fig. 5** Bit design. **a** Guide hole drilling tool. Used to grind the bottom of the hole into a conical shape with upper and lower diameters of 85 mm and 50 mm. **b** Measuring hole drilling tool. Used to continue drilling a measuring hole that meets the requirements at the bottom of the conical hole. In addition, there are two diameter specifications, 40 mm and 50 mm, with a maximum drilling depth of 600 mm

rotate the inner tube and cut rocks during the drilling process with the outer tube. Further reduce the destructive effect of mechanical force (longitudinal and transverse vibration produced by drilling tools) on the core. According to the characteristics of double-tube drilling tool and the requirements of downhole operation in the process of in-situ stress measurement. Different drill bits matching with the operation task are designed, and double-tube guide hole drilling tool, double-tube measuring hole drilling tool and double-tube stress relief hole drilling tool are formed. In addition, the flow passage and coring mode are also optimized. The optimized drilling tool has the advantages of accurate hole forming and stable coring, and assists in the rapid measurement of in-situ stress.

#### 3.2.1 Design of High-Quality Hole Forming

Before drilling the measuring hole, it is necessary to grind a guide hole with conical surface at the hole bottom, and then the measuring hole bit enters the hole bottom along the conical surface. The guide hole can centralize the measuring hole bit and locate the drilling direction. As shown in Fig. 5a, the included angle between the inclined lip of the guide hole bit and the vertical direction of drilling is  $A^\circ$ , the included angle between the inclined edge of the clamping jaw and the drilling direction is  $B^\circ$ , and  $A^\circ + B^\circ = 90^\circ$ . This design avoids the severe collision between the clamping jaw and the hole wall and damaging the ring breaking conical hole bottom. In addition, the pump pressure rise after the clamping jaw contacts the conical surface can be used as the judgment basis for the completion of guide hole drilling. The lip

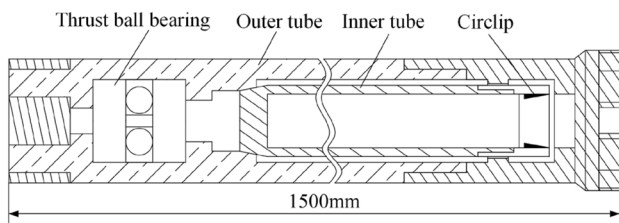


**Fig. 6** Single acting double-tube drilling tool for stress relief hole. The outer tube of the drilling tool drives the drill bit to cut rocks, while the inner tube does not rotate, ensuring that the rock core and measurement equipment entering the inner tube are not disturbed by drilling. The total length of the drilling tool is 1500 mm, and the maximum core drilling depth is 1200 mm

surface of the measuring hole bit adopts the annular groove diamond design, and the middle of the lip surface is concave inward, as shown in Fig. 5b. During the drilling process, the raised annular groove drilling teeth mesh with the annular groove formed by cutting the rock at the bottom of the hole to ensure that the measuring hole bit always drills in a stable direction. Moreover, the concave bit lip and convex core further limit the swing of the bit. In addition, the concave design of the bit lip and raised core further limited bit swing.

### 3.2.2 Design of Flow Passage

Since the measuring hole bit is concave design, it is easy to cause rock debris accumulation in the middle of the bit and affect the drilling effect. As shown in Fig. 5, a water outlet is arranged near the center of the measuring hole bit. The water outlet can effectively flush away the accumulated rock cuttings to ensure smooth drilling. At the same time, it can also cool the bit to avoid overheating, which will affect the hole forming accuracy. During the coring drilling of stress relief hole, the drilling fluid flows through the thrust ball bearing from the drill pipe, and then flows to the stress relief hole bit from the channel between the outer tube and the inner tube of the drill tool. It does not directly flow through the inner tube of the drill tool, so as to avoid the measurement error caused by the direct scouring of the measurement equipment by the drilling fluid.

### 3.2.3 Design of Coring

In-situ stress measurement should be carried out in the complete rock core. If the core is cut off due to rotation, it will cause the failure of in-situ stress measurement. Figure 6 shows a single acting double-tube stress relief hole drilling tool. A thrust ball bearing is set at the connection between the inner and outer tube. One end of the inner tube is connected with the thrust ball bearing and the other end

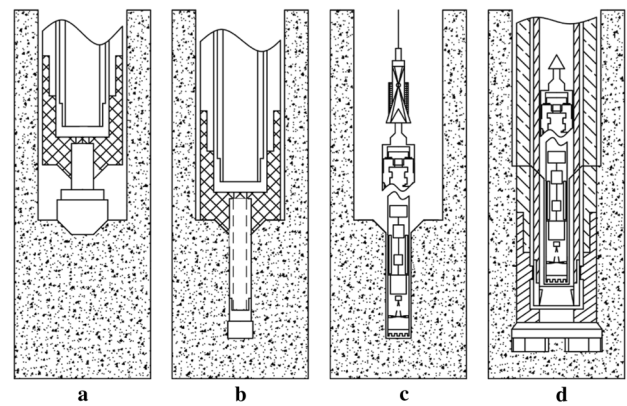


**Fig. 7** Schematic diagram of downhole operation. **a** Drilling guide hole with conical surfaces. **b** Drilling measuring hole for installing measurement equipment. **c** Installing the measurement equipment into the measuring hole through the coordination of conventional fishing tools and spear. **d** Drilling and recovering the core and measurement equipment

is connected with the circlip. In the process of stress relief hole drilling, the diametrical deformation measurement equipment and core enter the inner tube of the drilling tool through the circlip. The drill pipe drives the outer tube of the drilling tool to rotate and drives the stress relief hole bit to cut rock. The thrust ball bearing limits the rotation of the inner tube, realizes the separation of the power system and the measurement system, and protects the core and diametrical deformation measurement equipment.

### 3.3 In-Situ Stress Measurement Process

In order to complete the downhole operation tasks shown in Fig. 7, a set of scientific and standardized in-situ stress measurement process is developed:

- (1) Lower the double-tube guide hole drilling tool to the hole bottom, clean the residual core and grind it to form a conical hole bottom;
- (2) Recover the double-tube guide hole drilling tool, replace and lower the double-tube measuring hole drilling tool to the hole bottom, drill the measuring hole, and the designed drilling footage is 50 cm;
- (3) Recover the double-tube measuring hole drilling tool, lower and install the diametrical deformation measurement equipment into the measuring hole;
- (4) Replace and lower the double-tube stress relief hole drilling tool to the hole bottom, and conduct coring drilling for the measuring hole. The designed drilling footage shall not be less than 60 cm;

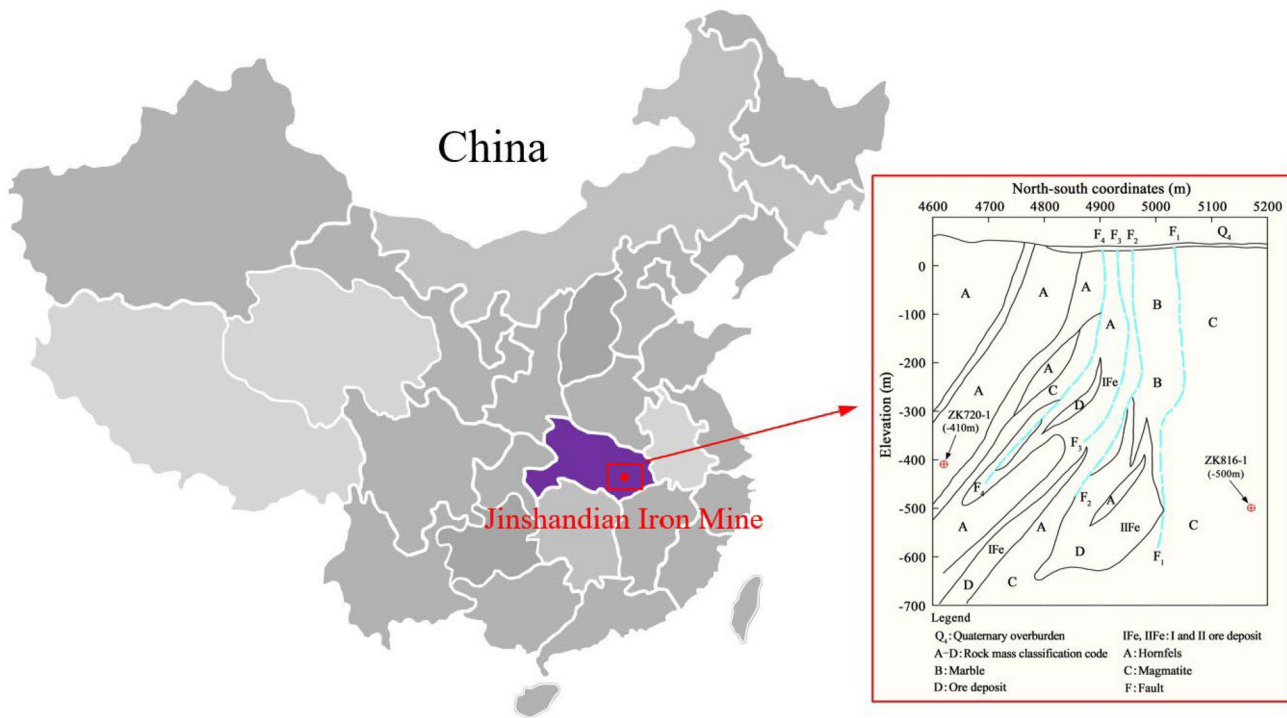


**Fig. 8** Location and geological profile of the mine area

- (5) Recover the double-tube stress relief hole drilling tool, take out the core and diametrical deformation measurement equipment, and observe whether the core is complete. If the core is complete, the measurement is completed. If it is incomplete, repeat steps (1) to (5) until the complete core is taken out.

## 4 In-Situ Measurement and Results

### 4.1 Test Project Overview

Zhangfushan deposit of Jinshandian Iron Mine is an important ore production base of Wuhan Iron and steel group company, the location and geological profile of the mine area are shown in Fig. 8. It is 3500 m long from east to west, 1000 m wide from north to South and covers an

**Fig. 9** Auxiliary measurement equipment and diametrical deformation measurement equipment





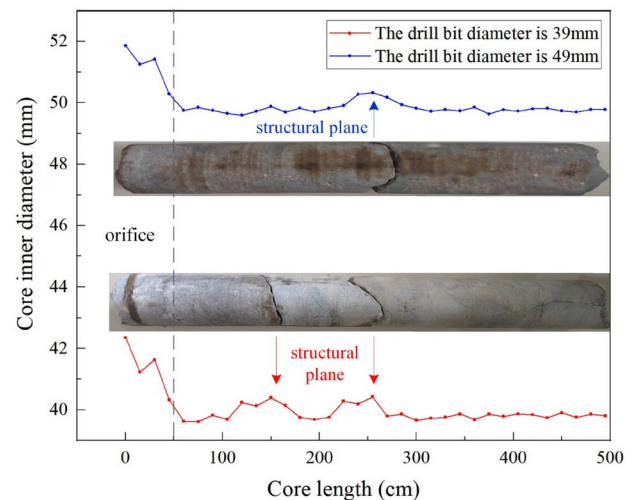
**Table 1** Basic information of in-situ stress measurement

Borehole	Buried depth (m)	Measuring point depth (m)	Measurement time	Measurement result
<b>ZK720-1</b>	<b>480.78</b>	<b>26</b>	<b>1 h 24 min</b>	<b>Core breaks during drilling</b>
ZK720-1	488.78	34	1 h	Rock fragmentation
ZK720-1	491.78	37	–	Rock fragmentation
ZK720-1	507.38	52.6	1 h 52 min	Rock fragmentation
<b>ZK720-1</b>	<b>508.38</b>	<b>53.6</b>	<b>1 h 17 min</b>	<b>Obtain deformation data</b>
ZK816-1	566.47	23.7	1 h 54 min	Measuring point is close to the structural plane
ZK816-1	567.37	24.6	1 h 23 min	Measuring point is close to the structural plane
ZK816-1	568.07	25.3	54 min	Fracture zone
ZK816-1	569.27	26.5	1 h 15 min	Fracture zone
<b>ZK816-1</b>	<b>575.17</b>	<b>32.4</b>	<b>1 h 30 min</b>	<b>Core breaks during drilling</b>
<b>ZK816-1</b>	<b>575.97</b>	<b>33.2</b>	<b>1 h 18 min</b>	<b>Obtain deformation data</b>
<b>ZK816-1</b>	<b>576.67</b>	<b>33.9</b>	<b>1 h</b>	<b>Obtain deformation data</b>
<b>ZK816-1</b>	<b>577.37</b>	<b>34.6</b>	<b>1 h 1 min</b>	<b>Obtain deformation data</b>

area of about 3.5 km<sup>2</sup>. The eastern part of the deposit is greatly affected by fault tectonic movement and the lithology distribution is complex. The surrounding rock properties of roadway mainly include magmatite, fault fracture zone and hornfels. Magmatite exists in hornfels in the form of rock branch and vein, which is relatively complete, with high rock mass strength, and the rock mass quality rating result is grade II (Yang et al. 2020). Hornfels is relatively broken, the rock mass strength is low, and the rock mass quality rating is grade III; The fault runs through the whole area, with an attitude of about 183°∠55°~85°, steep at the top and gentle at the bottom, with a width of about 35 m. The typical geological profile model is shown in Fig. 8.

In this paper, two test boreholes zk720-1 and zk816-1 are arranged at – 410 m and – 500 m levels in the east area of Zhangfushan deposit. In-situ stress measurement tests are carried out while drilling. Figure 9 shows the auxiliary measurement equipment and diametrical deformation measurement equipment used in this paper. Boreholes zk720-1 and zk816-1 are far away from the fault, the depth of the measuring point (the depth from the in-situ stress measuring point to the orifice) is more than 3 times larger than the roadway span, and the measuring point is more than 30 m away from the adjacent roadway and other excavation works.

In this paper, in-situ stress measurements were carried out at 13 points in the two boreholes, as shown in Table 1. There are 5 measuring points in borehole zk720-1, and the depth of measuring points is between 26 and 53.6 m, of which the rock strata at 34 m, 37 m and 52.6 m are broken and the core is incomplete; There are 8 measuring points in borehole zk816-1, and the depth of measuring points is between 23.7 and 34.6 m. At 23.7 m and 24.6 m, the contact

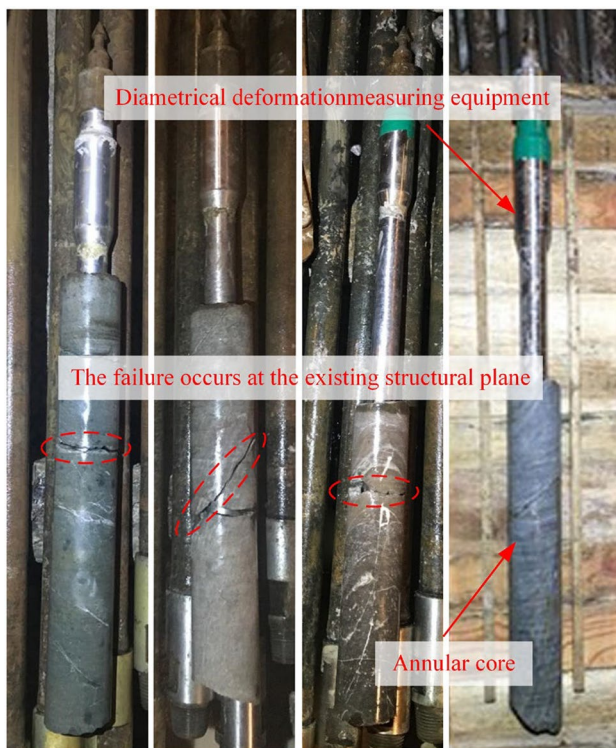


**Fig. 10** Statistics of inner diameter of some cores

pins of diametrical deformation measurement equipment are just near the structural plane, so the measurement data are unreliable. At 25.3 m and 26.5 m, the rock is broken and the core is incomplete. Therefore, the effective diametrical deformation data at 6 measuring points were obtained, which are shown in bold in Table 1. Among them, the core at 26 m in borehole zk720-1 and 32.4 m in borehole zk816-1 was damaged during coring, but the diametrical deformation data of the measuring hole before coring were obtained. The measurement time at 6 measuring points is between 1 and 1 h 30 min, and the average measurement time is 1 h 15 min. Compared with the conventional stress relief method, the measurement time in this paper is greatly reduced.

**Table 2** Integrity analysis of core

Borehole	Measuring point depth (m)	Coring depth (cm)	Core length (cm)	Core recovery (%)	RQD
ZK720-1	26	60	59.1	98.5	100%
ZK720-1	53.6	60	58.5	97.5	100%
ZK816-1	32.4	60	58.2	97	100%
ZK816-1	33.2	60	48.9	81.5	75%
ZK816-1	33.9	60	58	96.7	100%
ZK816-1	34.6	60	57.7	96.2	100%

**Fig. 11** Diametrical deformation measurement equipment and core

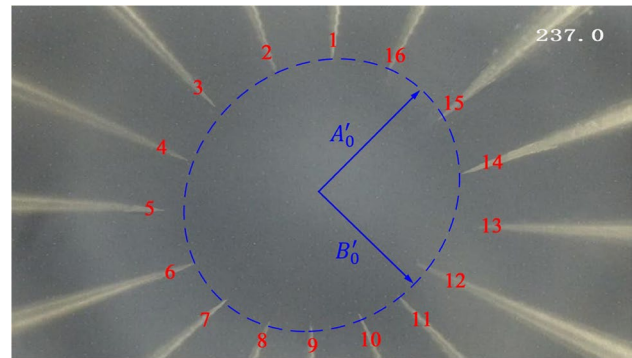
## 4.2 Analysis of Measurement Results

### 4.2.1 Analysis of Measuring Hole Accuracy

Although the centering design is considered in the drill bit, it will inevitably cause slight shaking in the process of cutting rock, so the borehole diameter will fluctuate in a certain range. Two different measuring drill bits with 49 mm and 39 mm diameters were used in borehole ZK720-1 and ZK816-1. The inner diameter of the core was measured with an inner diameter dial indicator every 15 mm, and the inner diameter distribution of each core was counted. Figure 10 shows the inner diameter distribution of core at 32.4 m of borehole zk816-1 and 26 m of borehole zk720-1. It can

**Table 3** Physical parameters of rock

Borehole	Lithology	Elastic modulus ( $\times 10^3$ MPa)	Poisson's ratio
ZK720-1	Hornfels	52.8	0.31
ZK816-1	Diorite porphyrite	41.1	0.26

**Fig. 12** Micro-optical image of contact pins before drilling stress relief hole at 26 m measuring point in borehole zk720-1

be seen from the figure that the inner diameter of annular lithology changes greatly at the orifice and near the structural plane. In the complete rock core away from the orifice and structural plane, the floating range of diameter is very small, and the maximum floating range is only 0.425 mm. The measuring range of the contact pins in each direction is 2.5 mm, and the floating range of the diameter is within the requirements of the diametrical deformation measurement equipment. Although the diameter of the measuring hole may fluctuate within a range, it will only affect the installation of the diametrical deformation measurement equipment and have a very small effect on the calculation results of in-situ stress. The effect on in-situ stress results will be explained later.

### 4.2.2 Analysis of Coring Integrity

In this paper, the drilling depth of the measuring hole is 50 cm, and the core drilling of the stress relief hole is 60 cm. In order to investigate the coring quality of double-tube stress relief hole drilling tool, the integrity of 6 groups of cores obtained is measured and analyzed, and the results are shown in Table 2. Figure 11 shows the core and diametrical deformation measurement equipment.

The core recovery rate and RQD at 33.2 m of borehole zk816-1 are lower due to rock fragmentation, and the core recovery rate at the other five measuring points are more than 96%, and the RQD is 100%. In addition, the core failure basically occurs near the existing structural plane. The

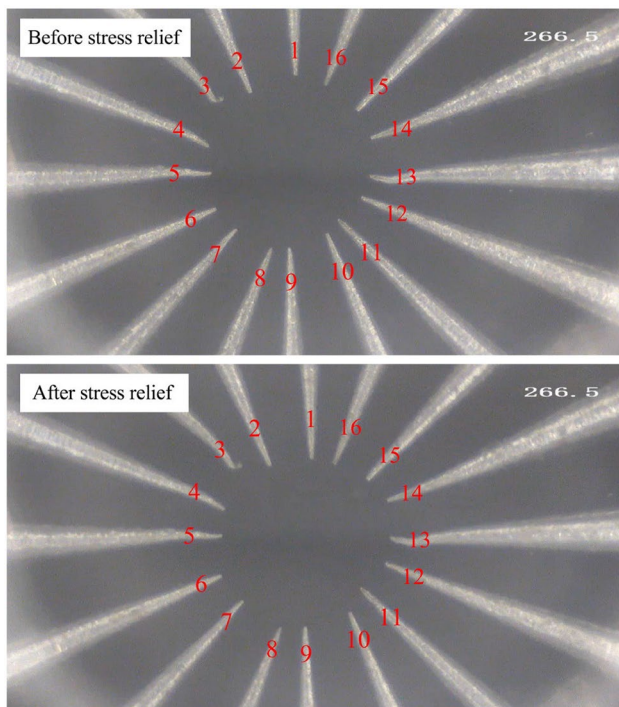


**Fig. 13** Micro-optical images of contact pins before and after stress relief at 53.6 m measuring point in borehole zk720-1

results show that the auxiliary measurement equipment has good coring performance.

#### 4.2.3 In-Situ Stress Calculation

For the measuring points that obtain the diametrical deformation data of core after stress relief, the stress state can be calculated by Eq. (6). In addition, for the measuring points that only obtain the diametrical deformation data of the measuring hole before coring, the stress state can be estimated by Eqs. (12) and (13). Taking the 26 m measuring point and 53.6 m measuring point in borehole zk720-1 as examples, the in-situ stress calculation processes are introduced, respectively. The physical parameters of rock are shown in Table 3.

1) Calculation process of in-situ stress at 26 m measuring point

The upper rock at 26 m measuring point in zk720-1 is relatively complete, and the core is broken during coring drilling. Figure 13 is the micro-optical image of the contact pins before drilling the stress relief hole. The rock strata at the measuring points in this paper are not magnetic, and the electronic compass can work normally. The orientation of No. 1 contact pin in the figure is  $237^\circ$ , and the orientation of other contact pin can be determined according to the rule of counterclockwise decreasing by  $22.5^\circ$ . Digital image processing (DIP) is a very mature technology to remove noise,

enhance, restore, segment and extract features of images through computers. The needle tip coordinates of each contact pins can be accurately identified by DIP technology. According to the basic principle of least square method, the general equation of ellipse is fitted from the needle tip coordinates, as shown in Fig. 12. The semimajor axis of the ellipse  $A'_0 = 1.346\text{mm}$ , and the direction is  $91.9^\circ$ . The semiminor axis of the ellipse  $B'_0 = 1.326\text{mm}$ , and the direction is  $1.9^\circ$ . Therefore, the direction of the maximum horizontal principal stress is  $\alpha = 1.9^\circ$ .

Since the length of the contact pin is 24.750 mm, the section ellipse semimajor axis is  $A_0 = 26.096\text{mm}$  and ellipse semiminor axis is  $B_0 = 26.076\text{mm}$  after borehole deformation. Although the ellipse shape parameters after borehole deformation are obtained by contact pins displacement, it is difficult to obtain the initial diameter of borehole accurately. It can be seen from Eqs. (12) and (13) that the initial diameter of the borehole has a great influence on the calculation results of the principal stress, but has little influence on the differential stress. For example, when the initial diameter of the borehole is 52.140 mm, the maximum horizontal principal stress is  $\sigma_H = 23.56\text{MPa}$ , the minimum horizontal principal stress is  $\sigma_h = 12.12\text{MPa}$ , and the differential stress is  $S = 11.4385\text{MPa}$ . In addition, when the initial diameter of the borehole is 52.141 mm, the maximum horizontal principal stress is  $\sigma_H = 23.00\text{MPa}$ , the minimum horizontal principal stress is  $\sigma_h = 11.56\text{MPa}$ , and the differential stress is  $S = 11.4383\text{MPa}$ . It shows that the deviation of principal stress caused by borehole diameter error at this measuring point is  $0.56\text{Mpa}/\text{um}$ , while the deviation of differential stress is only  $0.0002\text{Mpa}/\text{um}$ . The initial diameter of the borehole is affected by the drilling procedure, as shown in Fig. 10. The maximum error of the measuring hole diameter in this paper reaches 0.425 mm. The principal stress deviation caused by this error is 238 Mpa, while the differential stress deviation is only 0.085 Mpa. Therefore, when the diameter of the measuring hole cannot be accurately controlled, the magnitude of the principal stress cannot be obtained, but the magnitude of the differential stress is acceptable. In this paper, the section ellipse minor axis is used to replace the initial diameter in the calculation, and the differential stress is calculated as  $S = 11.44\text{Mpa}$ .

2) Calculation process of in-situ stress at 53.6 m measuring point

The deformation data of core in the whole process of stress relief were obtained at the measuring point of 53.6 m in borehole ZK720-1. The total length of the diametrical deformation measurement equipment used in this paper is 854 mm. At the measuring point of 53.6 m, the insertion depth of the contact pins is 205 mm. Using digital image processing technology, analyze the micro-optical images collected in the whole process of stress relief, identify and



**Fig. 14** Diametrical deformation curve of core at 53.6 m measuring point in borehole zk720-1

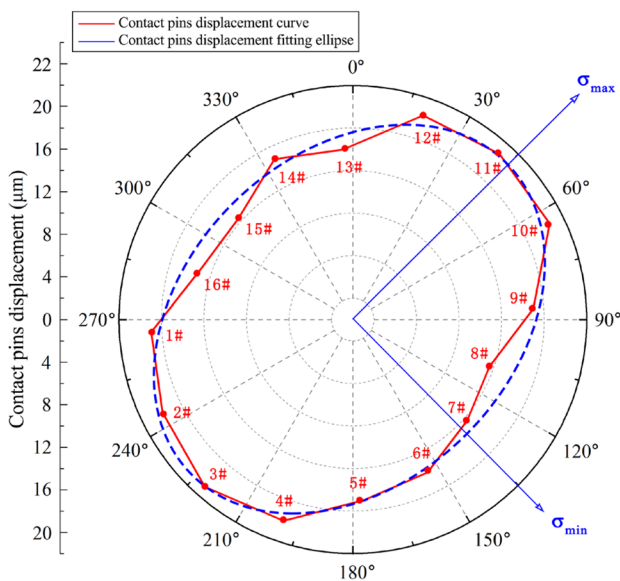
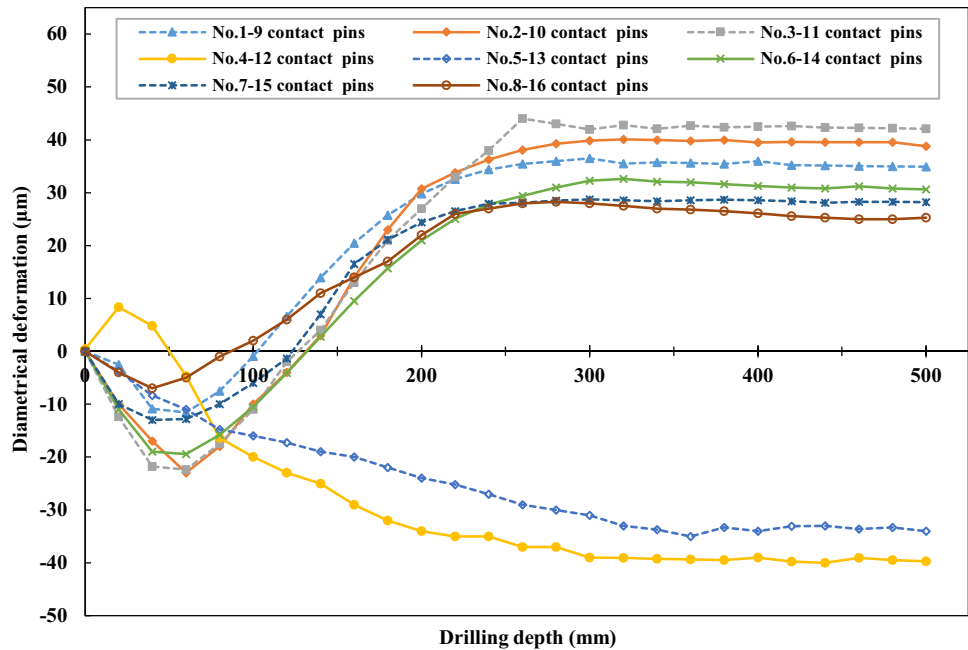


**Fig. 15** Fitting of contact pins displacement

calculate the displacement of each contact pins. Figure 14 shows the micro-optical images of the contact pins before and after stress relief. As shown in Fig. 13, the azimuth of No. 1 contact pin is  $266.5^\circ$ , and the azimuth of other contact pins can be determined according to the rule of decreasing  $22.5^\circ$  counterclockwise. Figure 14 shows the deformation curve of borehole diameter in 8 directions. When the drilling depth is greater than 205 mm, the borehole diameter deformation is gradually stable. Except for No. 4-12 contact pins ( $19^\circ$ ) and No. 5-13 contact pins ( $176.5^\circ$ ), the variation law

of most diametrical deformation curves is reasonable and the measured data are reliable.

It can be seen from Eq. (6) that the maximum and minimum principal stress values and principal stress directions in the plane can be calculated by the combination of diametrical deformation in any three directions. The error in Fig. 10 is much smaller than the borehole diameter, and the strain caused by the error is almost negligible, that is, it will not affect the calculation of in-situ stress. After excluding some unreasonable deformation data, the displacement, azimuth data and rock physical parameters of different combinations are brought into Eq. (6). It is calculated that the average maximum horizontal principal stress at this point is  $\sigma_H = 25.18 \text{ MPa}$ , the average minimum principal stress is  $\sigma_h = 20.77 \text{ MPa}$ , and the direction of the maximum horizontal principal stress is  $\alpha = 48.8^\circ$ .

The diametrical deformation in multiple directions can accurately describe the morphological characteristics of the core section after stress relief. By fitting the displacement of 16 contact pins at 53.6 m in borehole zk720-1, the elliptical shape of the core section after deformation is obtained, as shown in Fig. 15, and the direction of principal stress can be quickly judged through the morphological characteristics of the ellipse. The semimajor axis of the ellipse represents the direction of maximum horizontal principal stress, and the semimajor axis represents the direction of minimum horizontal principal stress. It can be seen from Fig. 16 that the maximum horizontal principal stress direction is about  $45^\circ$  and the minimum principal stress direction is about  $135^\circ$ , which is consistent with the calculated results. The in-situ stress measurement results at the 6 measuring points in this paper are shown in Table 4.



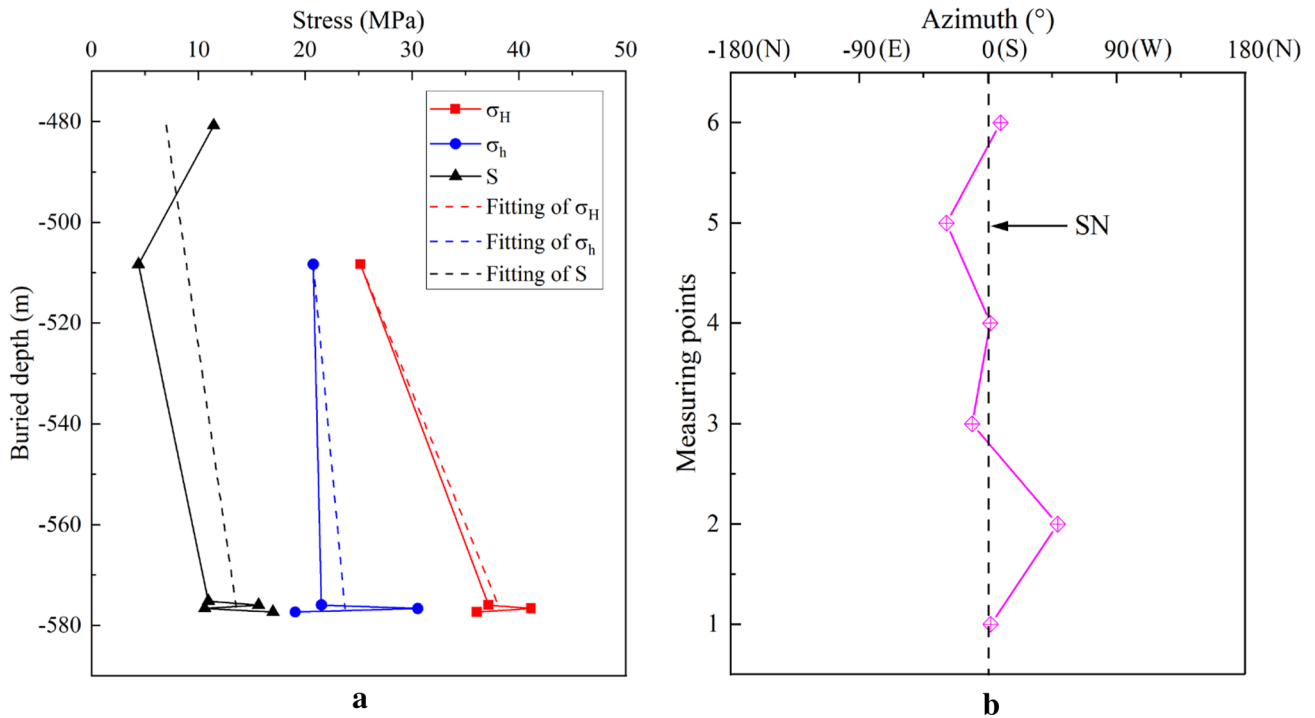


Fig. 16 Magnitude and azimuth of in-situ stress with depth. a Magnitude. b Azimuth of the horizontal maximum principal stress

Table 4 In-situ stress calculation results

Borehole	Buried depth (m)	Measuring point depth (m)	$\sigma_H$ (MPa)	$\sigma_h$ (MPa)	S (MPa)	$\alpha$ (°)
ZK720-1	480.78	26	/	/	11.44	1.9
ZK720-1	508.38	53.6	25.18	20.77	4.41	48.8
ZK816-1	575.17	32.4	/	/	10.94	169.2
ZK816-1	575.97	33.2	37.16	21.53	15.63	1.6
ZK816-1	576.67	33.9	41.15	30.55	10.6	151.3
ZK816-1	577.37	34.6	36.08	19.09	16.99	8.8

In the table,  $\sigma_H$  and  $\sigma_h$  are the maximum horizontal principal stress and minimum horizontal principal stress perpendicular to the drilling axis, respectively;  $S$  is differential stress;  $\alpha$  is the direction of maximum horizontal principal stress. The measurement results indicate that, the magnitude of stress basically increases with depth, as shown in Fig. 16a. The value of  $\sigma_H$  increases with depth by approximately 0.19 MPa/m,  $\sigma_h$  by approximately 0.043 MPa/m, and  $S$  by approximately 0.068 MPa/m. Due to the close burial depth of the measurement points in borehole ZK816-1, the fitting curve uses the measurement data from borehole ZK720-1 and the average of the measurement data from borehole ZK816-1. The maximum horizontal principal stress direction obtained from different measurement points is not exactly the same, but fluctuates near the SN direction, as shown in Fig. 16b. The reasons for the differences may be measurement uncertainty or natural changes in stress state. But the average value of the maximum

horizontal principal stress direction at the six measuring points is very close to SN.

### 5 Discussion

The in-situ stress measurement method proposed in this paper includes two forms. If the core is complete, the stress state can be accurately calculated by borehole diametrical deformation after coring. If the core is incomplete, the stress state can be estimated by the cross-sectional shape parameters of the borehole before coring. Limited by the accurate acquisition of the initial diameter of the borehole, the principal stress calculated by the borehole cross-sectional shape analysis has a certain error, but the differential stress and the direction of the principal stress are accurate. The cross-sectional shape of the borehole

before coring and diametrical deformation of the borehole after coring can be obtained continuously in one measurement process, and the appropriate in-situ stress calculation method can be selected according to whether the core is complete. Funato and Ito (2017) proposed a new method of diametrical core deformation analysis (DCAD) for in-situ stress measurements. This method calculates the differential stress by measuring the shape of the core after deformation, and the direction of the principal stress can also be obtained if the core is oriented. In contrast, the method proposed in this paper can realize the directional measurement of borehole section in the field, and can obtain the differential stress and the direction of principal stress more quickly without relying on the core.

In the application case of this paper, there are few in-situ stress measurement data in Zhangfushan deposit area. Chen (2004) gives the in-situ stress measurement data of this deposit at the buried depth of 60 m and 307 m. The maximum principal stress at the buried depth of 307 m is 15.79 Mpa and the direction is  $196.26^\circ$ . According to the geotectonic position and characteristics of the mining area, as well as the existing structural traces and characteristics, he speculated that the maximum principal stress direction of the existing structural stress in the mining area is near SN or NNE–SSW. The direction of maximum principal stress at five of the six measurement points in this paper is nearly SN, and the other one is slightly deflect, which is basically consistent with the existing data, indicating that the measurement results in this paper are reliable.

## 6 Conclusion

In this paper, an in-situ stress measurement method based on borehole diametrical deformation analysis is proposed. The calculation principle of in-situ stress is established and the corresponding measurement equipment is developed. In addition, the field measurement of in-situ stress has been carried out. The main conclusions are as follows:

- (1) The analysis of borehole diametrical deformation under stress is deduced, and two methods to calculate in-situ stress by measuring borehole diametrical deformation and borehole cross-sectional shape are established.
- (2) The borehole diametrical deformation measurement equipment is developed, it realizes multi-directional diametrical deformation measurement by using key components such as rigid measuring contact pins, CCD camera and electronic compass. The equipment can withstand pressure of 15 MPa and temperature of  $100^\circ\text{C}$  and can meet the measurement requirements of complex environment in deep hole. Moreover, it is easy to install and does not need to be bonded with the hole

wall, which simplifies the operation process of in-situ stress measurement.

- (3) In order to complete the downhole operation task of in-situ stress measurement, the traditional single action double-tube drilling tool is optimized to meet the drilling requirements of accurate hole forming and complete coring. Thus, a set of rapid in-situ stress measurement technology with the cooperation of aperture deformation measurement device and drilling tool is formed.
- (4) The method proposed in this paper is applied to the in-situ stress measurement at  $-410$  m and  $-500$  m levels in Jinshandian Iron Mine, and the borehole diametrical deformation data at 6 measuring points are obtained. The core collected by the optimized drilling tool has stable inner diameter and high coring integrity, and the average time of each measuring point is only 1 h 15 min. The value of principal stress basically increases with the increase of depth, and the direction of the maximum horizontal principal stress is about SN, which is basically consistent with the existing in-situ stress data.

**Acknowledgements** This work was supported by the National Natural Science Foundation of China (Grant Nos. 41731284 and 41902294).

**Author Contributions** CW: methodology, data curation, investigation, writing—original draft. ZH: supervision, project administration, writing—review and editing. YW: methodology, investigation, writing—original draft. CW: conceptualization, formal analysis. JW: funding acquisition, software. SH: project administration, resources.

**Data availability** Data will be made available on request.

## Declarations

**Conflict of Interest** The authors declare that they have no known competing financial interests or personal relationships that could have appeared to influence the work reported in this paper.

## References

- Bai JP, Hua P, Ma XM, Jiang JJ, Li Z (2013) Hollow inclusion strain gauge geostress measuring instrument in deep borehole and its application example. *Chin J Rock Mech Eng* 32:902–908 (**in Chinese**)
- Bai X, Zhang DM, Wang H, Li SJ, Rao Z (2018) A novel in situ stress measurement method based on acoustic emission Kaiser effect: a theoretical and experimental study. *R Soc Open Sci* 5:181263
- Byrne TB, Lin W, Tsutsumi A, Yamamoto Y, Lewis JC, Kanagawa K, Kitamura Y, Yamaguchi A, Kimura G (2009) Anelastic strain recovery reveals extension across SW Japan subduction zone. *Geophys Res Lett* 36:L23310
- Cai MF, Qiao L, Yu J (1995) Study and tests of techniques for increasing overcoring stress measurement accuracy. *Int J Rock Mech Min Sci Geomech. Abstr* 32:375–384

- Cai MF, Qiao L, Yu B, Wang SH (2000) Stress measurement with an improved hollow inclusion technique In Jinchuan Nickel Mine. *J Univ Sci Tech Beijing* 7:157–160
- Chen CX (2004) A study of stability of underground mining in complex conditions, PhD Thesis. The Chinese Academy of Sciences (Institute of Rock and Soil Mechanics), Wuhan, China (in Chinese)
- Feng XT, Zhou YY, Jiang Q (2019) Rock mechanics contributions to recent hydroelectric developments in China. *J Rock Mech Geotech Eng* 11:511–526
- Funato A, Ito T (2017) A new method of diametrical core deformation analysis for in-situ stress measurements. *Int J Rock Mech Min Sci* 91:112–118
- Ge XR, Hou MX (2012) Principle of in-situ 3D rock stress measurement with borehole wall stress relief method and its preliminary applications to determination of in-situ rock stress orientation and magnitude in Jinping hydropower station. *Sci China Technol Sci* 55:939–949
- Haimson BC, Cornet FH (2003) ISRM suggested methods for rock stress estimation—part 3: hydraulic fracturing(HF) and/or hydraulic testing of pre-existing fractures(HTPF). *Int J Rock Mech Min Sci* 40:1011–1020
- Han ZQ, Wang CY, Wang C, Zou XJ, Jiao YY, Hu S (2020a) A proposed method for determining in-situ stress from borehole breakout based on borehole stereo-pair imaging technique. *Int J Rock Mech Min Sci* 127:104215
- Han ZQ, Wang CY, Wang YT, Wang C (2020b) Borehole Cross-sectional shape analysis under in situ stress. *Int J GeoMech* 20:04020045
- He BG, Hatzor Y (2015) An analytical solution for recovering the complete in-situ stress tensor from Flat Jack tests. *Int J Rock Mech Min Sci* 78:18–126
- Lahaie F, Gunzburger Y, Ben Ouanas A, Barnichon JD, Bigarre P, Piguet JP (2010) Impact of epoxy glue curing time on the quality of overcoring stress measurements in low-temperature environments. In: 5th International Symposium on In-Situ Rock Stress. Beijing, China, pp 161–166
- Layer E (1997) Measuring system for monitoring the rock mass stress. *Measurement* 22:57–68
- Leeman ER (1971) The CSIR “doorstopper” and triaxial rock stress measuring instruments. *Rock Mech Rock Eng* 3:25–50
- Lehtonen A, Cosgrove JW, Hudson JA, Johansson E (2012) An examination of in situ rock stress estimation using the Kaiser effect. *Eng Geol* 124:2–37
- Li CC (2021) Principles and methods of rock support for rockburst control. *J Rock Mech Geotech Eng* 13:46–59
- Li Y, Tang DZ, Xu H, Yu TX (2014) In-situ stress distribution and its implication on coalbed methane development in Liulin Area, Eastern Ordos Basin, China. *J Petrol Sci Eng* 122:488–496
- Li Y, Fu SS, Qiao L, Liu ZB, Zhang YH (2019) Development of twin temperature compensation and high-level biaxial pressurization calibration techniques for CSIRO in-situ stress measurement in Dept. *Rock Mech Rock Eng* 52:1115–1131
- Liu YQ, Li HB, Luo CW, Wang XC (2014) In situ stress measurements by hydraulic fracturing in the Western Route of South to North Water Transfer Project in China. *Eng Geo* 168:114–119
- Mckenney AM, Corkum AG (2020) Experimental evaluation of rapid flat jack testing with various shaped saw-cut slots. *Rock Mech Rock Eng* 53:455–466
- Merrill RH (1967) Three-component borehole deformation gage for determining the stress in rock. US Department of the Interior, Bureau of Mines, USA
- Mukai A, Yamauchi T, Ishii H, Matsumoto S (2007) In-situ stress measurement by the stress relief technique using a multi-component borehole instrument. *Earth Planets Space* 59:133–139
- Nagano Y, Lin WR, Yamamoto K (2015) In-situ stress analysis using the anelastic strain recovery (ASR) method at the first offshore gas production test site in the eastern Nankai Trough, Japan. *Mar Pet Geol* 66:418–424
- Oreste P (2005) Back-analysis techniques for the improvement of the understanding of rock in underground constructions. *Tunn Undergr Space Technol* 20:7–21
- Pang XQ, Jia CZ, Wang WY (2015) Petroleum geology features and research developments of hydrocarbon accumulation in deep petroliferous basins. *Petrol Sci* 12:1–53
- Ptacek J, Konicek P, Stas L, Waclawik P, Kukutsch R (2015) Rotation of principal axes and changes of stress due to mine-induced stresses. *Can Geotech J* 52:1440–1447
- Segawa M, Kimura M, Ooi K, Sugi S (1995) A micro-miniaturized ccd color camera utilizing a newly developed ccd packaging technique. *IEEE Trans Consumer Electron* 41:946–953
- Sjöberg J, Klasson H (2003) Stress measurements in deep boreholes using the Borre (SSPB) probe. *Int J Rock Mech Min Sci Geomech Abstr* 40:1205–1223
- Sjöberg J, Christiansson R, Hudson JA (2003) ISRM Suggested Methods for rock stress estimation—part 2: overcoring methods. *Int J Rock Mech Min Sci* 40:999–1010
- Sun DS, Lin WR, Cui JW, Wang HC, Chen QC, Ma YS, Wang LJ (2014) Three-dimensional in situ stress determination by anelastic strain recovery and its application at the Wenchuan Earthquake Fault Scientific Drilling Hole-1 (WFS-1). *Sci China Earth Sci* 57:1212–1220
- Talalay PG (2014) Foundations of drilling engineering. Geological Publishing House, Beijing
- Tang FL, Kalinin AG, Duan LC (2009) Core drilling science. China University of Geosciences Press, Wuhan (in Chinese)
- Vazaios I, Vlachopoulos N, Diederichs MS (2019) Assessing fracturing mechanisms and evolution of excavation damaged zone of tunnels in interlocked rock masses at high stresses using a finite-discrete element approach. *J Rock Mech Geotech Eng* 11:12–37
- Wang CY, Wang YT, Han ZQ, Wang JC, Zou XJ (2018) A system for measuring borehole diametric deformation based on mechanical contact and micro-optical imaging. *Measurement* 130:191–197
- Xie HP, Konietzky H, Zhou HW (2019) Special issue “deep mining.” *Rock Mech Rock Eng* 52:1415–1416
- Xu HJ, Sang SX, Yang JF, Jin J, Hu YB, Liu HH, Ren P, Gao W (2016) In-situ stress measurements by hydraulic fracturing and its implication on coalbed methane development in Western Guizhou, SW China. *J Unconv Oil Gas Resour* 15:1–10
- Yang KY, Chen CX, Xia KZ, Song XG, Zhang W, Zhang CQ, Wang TL (2020) Fault effect on the failure mechanism of surrounding rock in metal mine roadway by caving method. *Rock Soil Mech* 41:279–289
- Zhang XS, Wang HJ, Ma F, Sun XC, Zhang Y, Song ZH (2016) Classification and characteristics of tight oil plays. *Petrol Sci* 13:18–33
- Zhang H, Yin SD, Aadnoy B (2018) Poroelastic modeling of borehole breakouts for in-situ stress determination by finite element method. *J Petrol Sci Eng* 162:674–684

**Publisher's Note** Springer Nature remains neutral with regard to jurisdictional claims in published maps and institutional affiliations.

Springer Nature or its licensor (e.g. a society or other partner) holds exclusive rights to this article under a publishing agreement with the author(s) or other rightsholder(s); author self-archiving of the accepted manuscript version of this article is solely governed by the terms of such publishing agreement and applicable law.